Optical tuning of dielectric nanoantennas for thermo-optically reconfigurable nonlinear metasurfaces

MICHELE CELEBRANO[1], DAVIDE ROCCO[2,3,*], MARCO GANDOLFI[3,2], ATTILIO ZILLI[1], FRANCESCO RUSCONI[1], ANDREA TOGNAZZI[2], ANDREA MAZZANTI[1], LAVINIA GHIRARDINI[1], EVA A. A. POGNA[4,1], LUCA CARLETTI[2,3], CAMILLA BARATTO[3], GIUSEPPE MARINO[5], CARLO GIGLI[5], PAOLO BIAGIONI[1], LAMBERTO DUÒ[1], GIULIO CERULLO[1], GIUSEPPE LEO[5], GIUSEPPE DELLA VALLE[1,6], MARCO FINAZZI[1], AND COSTANTINO DE ANGELIS[2,3]

[1] Dipartimento di Fisica - Politecnico di Milano, Piazza Leonardo da Vinci, 32, I-20133 Milano, Italy
[2] Dipartimento di Ingegneria dell'Informazione, Università di Brescia, Via Branze 38 - 25123, Brescia, Italy
[3] Istituto Nazionale di Ottica, Consiglio Nazionale delle Ricerche, Via Branze 45 - 25123, Brescia, Italy
[4] NEST, Istituto Nanoscienze - CNR and Scuola Normale Superiore, 56127 Pisa, Italy
[5] Matériaux et Phénomènes Quantiques, Université de Paris, 10 rue Alice Domon et Léonie Duquet, 75013 Paris, France
[6] Istituto di Fotonica e Nanotecnologie, Consiglio Nazionale delle Ricerche, Piazza Leonardo da Vinci, 32, I-20133 Milano, Italy
* Corresponding author: davide.rocco@unibs.it

We demonstrate optically tunable control of second-harmonic generation in all-dielectric nanoantennas: by using a control beam which is absorbed by the nanoresonator, we thermo-optically change the refractive index of the radiating element to modulate the amplitude of the second-harmonic signal. For a moderate temperature increase of roughly 40 K, modulation of the efficiency up to 60% is demonstrated; this large tunability of the single meta-atom response paves the way to exciting avenues for reconfigurable homogeneous and heterogeneous metasurfaces. © 2021 Optical Society of America

1. INTRODUCTION

In the last two decades, metamaterials, artificial media where electromagnetic features can be engineered by designing the geometry of elementary building blocks called meta-atoms, have attracted a great interest in the scientific community in the quest for molding the properties of light beyond what was previously possible [1, 2]. The special case of metasurfaces, i.e. 2D metamaterials, owing to their planar profiles, is particularly appealing due to the simplified fabrication process compared to the 3D case and the long-sought promise for integration with on-chip nanophotonic devices [3]. Metasurfaces based on dielectric meta-atoms have recently witnessed tremendous advancements thanks to several key features, such as the possibility to obtain electric and magnetic Mie resonances and their low dissipative losses throughout the visible and infrared spectrum [4–6].

Dielectric metasurfaces have been recognized as an innovative platform for nonlinear optics, where new paradigms have

been introduced in the last years [7, 8]. Using a silicon platform, two orders of magnitude increase of third order nonlinear effects were first predicted in the seminal paper by Shcherbakov et al. [9]. Shortly after, second order nonlinearities were demonstrated in gallium arsenide platforms where record high Second Harmonic Generation (SHG) at the nanoscale was reported [10–13].

For the above reasons, nonlinear non-metallic metasurfaces are today at the forefront of research with three main challenges to be tackled first at the single meta-atom level: i) increase the efficiency of the nonlinear processes at the nanoscale also exploiting new concepts, such as anapoles and bound states in the continuum [8, 14–16]; ii) control and engineer the radiation pattern of the nonlinearly generated photons [17–19]; iii) tune and reconfigure the nonlinear emission to achieve all-optical modulation and multifunctional devices [20, 21]. As far as tunability and reconfigurability in the linear regime are concerned, many ideas have already appeared in the literature, involving, for example, the use of different stimuli (electrical, mechanical, optical and thermal) [22–24]. The challenge of reconfigurability in the nonlinear regime is now attracting a great deal of interest for basic science and applications [6, 25, 26].

In this work, we demonstrate control of SHG efficiency at the single meta-atom level in AlGaAs dielectric nanoantennas. The key concept is sketched in Fig. 1 (a) and (b): by changing the temperature of the nanoresonator, we can modulate the emitted second-harmonic (SH) signal. Once applied to an ensemble of meta-atoms, this idea straightforwardly translates into tunability of metasurfaces. Noteworthy, we demonstrate that the heating can be provided not only by a Peltier cell, but also all-optically by a control beam tuned above band-gap impinging on the nanoantenna. For a moderate temperature increase of roughly 40 K, modulation of the efficiency up to 60% is demonstrated in

a single nanoresonator; this large tunability of the meta-atom response paves the way to exciting avenues for all-optically reconfigurable nonlinear metasurfaces [27].

2. SHG TUNING

Since the first experiments on SHG from nanoantennas, it was immediately recognized that the properties of the emitted signal (e.g. efficiency, polarization and directionality) were strongly dependent on geometrical parameters (i.e. radius and height [28]). The experimental results are understood in terms of the optical size and geometry of the nanoresonator, which determine the spectral position of the resonances involved in the SHG process [29, 30]. Obviously, the optical size of an object can be modified by varying not only its physical dimensions, but also its refractive index.

With the aim of achieving reconfigurability, we exploit here the possibility of thermally tuning the refractive index to modulate the efficiency of the nonlinear process (Fig. 1a and 1b). Our experimental setup (described in the Supplementary) is a nonlinear confocal microscope: the excitation light (fundamental frequency, FF), delivered by a linearly polarized ultrafast Erbium-doped fiber laser centered at 1550 nm (160 fs pulse duration), is tightly focused to a diffraction-limited spot size of 1.8 μm onto the sample through a 0.85 numerical aperture air objective. The setup allows the interrogation of individual nanoparticles (NP) on the sample, where several pillars (3 μm apart from each other), with the same height (400 nm) and different radii (from 190 to 225 nm) have been fabricated to finely tune the nonlinear process with Mie resonances of the NP (see [11] for details of the fabrication procedure). For a FF pulse with peak intensity of 1 GW/cm^2, the dependence of the experimentally detected SHG on the NP radius is shown in Fig. 1c: as already reported in previous works [11], the most efficient SHG is obtained for specific radii and in the following we thus focus our attention only on five replicas of the five NPs with radius ranging from 195 nm to 215 nm (the region of the sample inside the white rectangle in Fig. 1c).

Our key idea is that the SH intensity can be modulated by the NP temperature. To demonstrate the principle, we consider two different means to control the NP temperature: (A) the sample is heated by a Peltier cell from room temperature T_0 to temperature $T_0 + \Delta T$; (B) the sample is heated by a light beam absorbed by the NP (a continuous wave (CW) pump of power P_p). In both cases, we quantify the SHG variation by the normalized differential signal:

$$\Delta SHG = \frac{I_{SHG}^{ON} - I_{SHG}^{OFF}}{I_{SHG}^{OFF}}, \quad \text{(1)}$$

where I_{SHG}^{ON} (I_{SHG}^{OFF}) is the SH light intensity generated by the NP when the external stimulus (either a Peltier cell or a light beam) is present (absent). Hence, I_{SHG}^{ON} is either a function of the temperature T set by the Peltier cell or a function of the optical control power P_p of the CW-pump. To rule out possible modulations due to linear effects, we have also characterized the linear optical contrast (see the Supplementary for the details).

A. THERMAL TUNING

In this case the NP is heated by a thermal contact: the nanoresonator's substrate adheres to a Peltier cell, set at a constant temperature $T_0 + \Delta T$ (Fig. 2c). The high thermal conductivity of the NP and of the GaAs wafer, as well as the homogeneity of
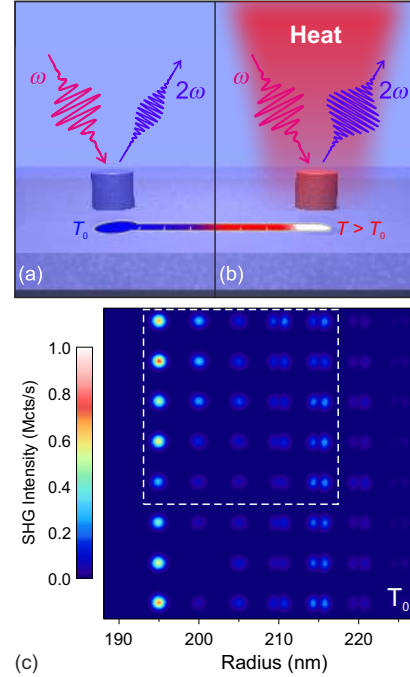

Fig. 1. (a) and (b): conceptual scheme of the controllable nonlinear antenna: the emitted SH can be modulated by a heat source. Panel (c): map of I_{SHG}^{OFF} collected at room temperature by a nonlinear microscope (described in the Supplementary), using a FF pulse with peak intensity of 1 GW/cm^2 from a sample with eight replicas (from top to bottom) of eight different pillars.

the AlOx substrate, results in an almost uniform temperature in the NP, close to $T_0 + \Delta T$ (see the Supplementary for the details).

Fig. 2(a) shows five replicas of the measured normalized differential SH signal ($\Delta SHG(T_0 + \Delta T)$) for $\Delta T = 20$ K. In Fig. 2b we summarize the previous findings by plotting $\Delta SHG(T_0 + \Delta T)$ for $\Delta T = 10$ K and $\Delta T = 20$ K. Note that, surprisingly, for a moderate temperature increase of 20 K, we observe large modulation (of about 20%) of the SHG efficiency. We then rationalize the experimental evidences in the frame of a thermo-optical model [31]. Following the same fitting procedure reported in [32], we describe the thermal AlGaAs refractive index change using the simplified relation $\Delta n(T, \lambda) = (dn/dT) \Delta T$. From the plot of dn/dT in Fig. 2c, we can appreciate that dn/dT is as low as few 10^{-4} K^{-1} at FF, and increases by orders of magnitude when approaching the band edge. This has a twofold relevance for our work: while an exact estimation of this parameter is beyond the main purpose of this Letter, we stress that large values of this parameter are crucial to obtain sizeable changes of the SH signal. Thus, engineering Mie resonances for efficient SHG at around the band edge of the semiconductor is the key point to obtain efficient modulation.

Our thermo-optical model computes numerically with COMSOL Multiphysics the SHG intensity variations due to thermally induced refractive index changes. By assuming $dn/dT \sim 10^{-3}$ K^{-1} (Fig. 2c), the ΔSHG value obtained by the model is in good agreement with the experimental results (Fig. 2d), proving that the physical reason for the observed modulation is the refractive index variation induced by the temperature change. The results reported in Fig. 2 show that a moderate uniform heating of the nanoantenna (up to 20 K) translates into an amplitude
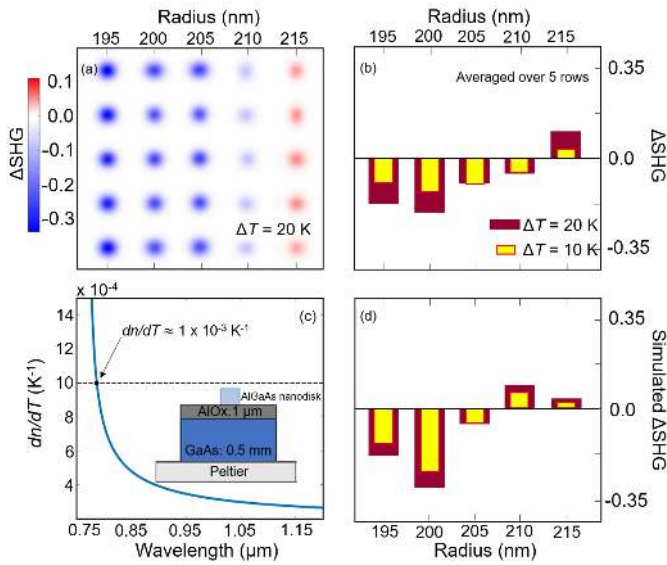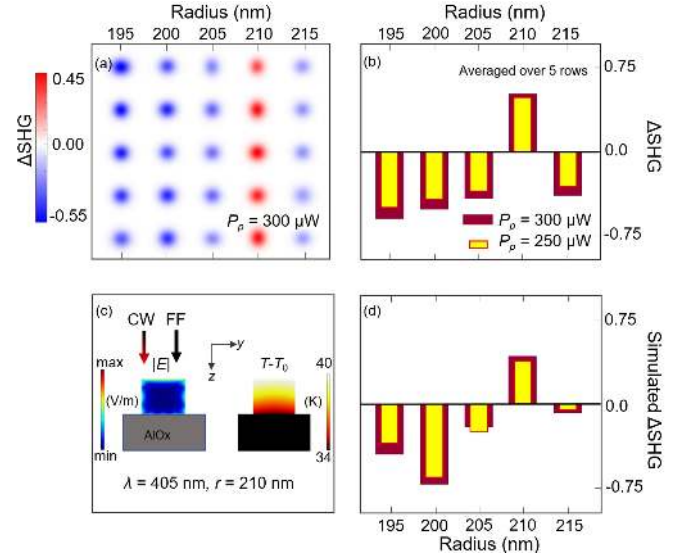
Fig. 2. (a) $\Delta SHG(T_0 + 20\,\text{K})$ measured on five replicas (from top to bottom) of five different nanopillars. The average of $\Delta SHG(T_0 + \Delta T)$ over each column in panel (a) is reported as red and yellow histograms in panel (b), for the five different radii and two different temperatures ($\Delta T = 10\,\text{K}$ and $\Delta T = 20\,\text{K}$) (c) Theoretical model of dn/dT versus wavelength. Inset: schematic of the Peltier cell heating. (d) Modeling data to be compared with the experimental data reported in panel (b).

Fig. 3. (a) Measured differential SH signal ($\Delta SHG(P_p)$) collected scanning five replicas of five different nanopillars with $P_p = 300\,\mu\text{W}$. (b) $\Delta SHG(P_p)$ for five different NPs radii for two control pump powers ($P_p = 250\,\mu\text{W}$ and $P_p = 300\,\mu\text{W}$). (c) Schematic of the optical heating (left) and induced temperature field in the NP (right) for a control pump power $P_p = 300\,\mu\text{W}$. (d) Modeling data to be compared with the experimental data reported in panel b).

modulation of the emitted SH intensity (up to 20%).

B. ALL-OPTICAL TUNING

Since the experimental results reported in Fig. 2 show that sizable modulations can be obtained with temperature changes of few degrees, we decided to explore the more appealing scenario of all-optical control, which allows addressing a single meta-atom within a metasurface. In this case, the heating is provided by the absorption of a control beam tightly focused on the nanoresonator. In order to heat the NP, we excite our structures with a CW pump beam (total power P_p focused on a spot size of 1 µm) at a wavelength $\lambda = 405$ nm, which is well above the bandgap of AlGaAs. Fig. 3(a) shows the map of five replicas of the experimentally measured normalized differential second harmonic signal ($\Delta SHG(P_p)$) for $P_p = 300\,\mu\text{W}$.

By comparing $\Delta SHG(P_p)$ (Fig. 3a) with $\Delta SHG(T)$ (Fig. 2a) we observe similar effects, which we can fully explain in the frame of an opto-thermo-optical model. We first estimate the effects of the CW control beam with an opto-thermal numerical simulation; the control beam hits the nanostructure, light is absorbed by the nanoresonator and in turn translates into a heat source that is responsible for the temperature increase (Fig. 3c). The numerical computation of the electric field within the NP discloses a non-homogeneous field confinement, yielding a strong light absorption at the top of the NP rather than in its center (Fig. 3c, left). In this case, heat diffusion gives rise to a moderate temperature gradient within the NP (Fig. 3c, right box). Hence, at variance with the scenario described in the previous section, here the non-uniform optical absorption leads to a non-uniform thermal heating; as a consequence, we experience a non-uniform refractive index, which is the reason for a different ΔSHG with respect to what we reported in the previous section. In Fig. 3b we summarize our experimental

findings by plotting $\Delta SHG(P_p)$ for $P_p = 250\,\mu\text{W}$ and $P_p = 300$ µW, corresponding to a maximum ΔT comparable to what we used in Fig. 2b. The ΔSHG obtained by our theoretical and numerical model is in good agreement with the experimental results (Fig. 3d).

We have also analyzed the all-optical tuning mechanism as a function of the control beam powers and for two different control beam wavelengths. The results are reported in Fig. 4, whose panels (a), (c) and (e) correspond to a control beam at $\lambda = 405$ nm, while panels (b), (d) and (f) correspond to a control beam at $\lambda = 532$ nm. From Fig. 4, we can see that the modulation depth can be changed by the input power of the control beam to obtain values as large as 60%. We also note that, at $\lambda = 532$ nm, our modelling (Fig. 4d) and our experimental results (Fig. 4b) show a decrease of the modulation depth above $P_p = 250$ µW. This is explained by a tuning of the nanoparticle big enough to go through the maximum of the resonance at SH. Furthermore, even if the AlGaAs absorption coefficient increases with frequency, the measured SHG modulation remains almost unchanged in the two considered cases. Indeed, as can be seen in Fig. 4f, the longer investigated wavelength experiences enhanced absorption due to excitation of higher order Mie resonances so that the overall absorption cross section of the NP is only slightly dependent on wavelength in this spectral region [10].

3. CONCLUSIONS

In conclusion, by using a strongly absorbed control beam that impinges on a nanoresonator, we have proven all-optical control of SHG in AlGaAs nanoantennas. The opto-thermally induced variation of the refractive index of the nanoresonator is used to modulate the amplitude of the emitted SH signal. Modulation of the efficiency up to 60% is experimentally demonstrated
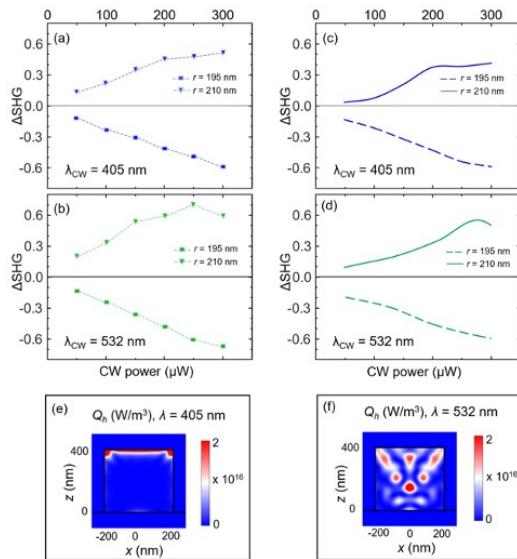
Fig. 4. Measured (a and b) and simulated (c and d) SHG modulation for two different pillar radii vs control beam power for a control wavelength of 405 nm (a and c) and 532 nm (b and d). Absorbed power density for a nanoresonator with radius 210 nm, excited with a control beam with power $P_p = 300$ µW and wavelength 405 nm (e) or 532 nm (f). In panels (a)–(d) positive (negative) modulation corresponds to a pillar radius of 210 nm (195 nm).

for a moderate temperature increase of about 40 K; such large tunability of the metasurface response at the single meta-atom level paves the way for all-optically reconfigurable nonlinear metasurfaces.

4. ACKNOWLEDGMENTS

5. DISCLOSURES.

The authors declare no conflicts of interest.

See Supplement 1 for supporting content.

REFERENCES

1. N. I. Zheludev and Y. S. Kivshar, Nat. Mater. **11**, 917 (2012).
2. M. Kadic, G. W. Milton, M. van Hecke, and M. Wegener, Nat. Rev. Phys. **1**, 198 (2019).
3. N. Yu and F. Capasso, Nat. Mater. **13**, 139 (2014).
4. A. I. Kuznetsov, A. E. Miroshnichenko, M. L. Brongersma, Y. S. Kivshar, and B. Lukyanchuk, Science **354**, aag2472 (2016).
5. Z. Zhou, J. Li, R. Su, B. Yao, H. Fang, K. Li, L. Zhou, J. Liu, D. Stellinga, C. P. Reardon, T. F. Krauss, and X. Wang, ACS Photonics **4**, 544 (2017).
6. I. Brener, S. Liu, I. Staude, J. Valentine, and C. L. Holloway, *Dielectric metamaterials: fundamentals, designs and applications* (1st ed. Woodhead Publishing, 2019).
7. A. Krasnok, M. Tymchenko, and A. Alù, Mater. Today **21**, 8 (2018).
8. K. Koshelev, S. Kruk, E. Melik-Gaykazyan, J.-H. Choi, A. Bogdanov, H.-G. Park, and Y. Kivshar, Science **367**, 288 (2020).
9. M. R. Shcherbakov, D. N. Neshev, B. Hopkins, A. S. Shorokhov, I. Staude, E. V. Melik-Gaykazyan, M. Decker, A. A. Ezhov, A. E. Miroshnichenko, I. Brener, A. A. Fedyanin, and Y. S. Kivshar, Nano Lett. **14**, 6488 (2014).
10. L. Carletti, A. Locatelli, O. Stepanenko, G. Leo, and C. De Angelis, Opt. Express **23**, 26544 (2015).
11. V. Gili, L. Carletti, A. Locatelli, D. Rocco, M. Finazzi, L. Ghirardini, I. Favero, C. Gomez, A. Lemaître, M. Celebrano, C. De Angelis, and G. Leo, Opt. Express **24**, 15965 (2016).
12. S. Liu, M. B. Sinclair, S. Saravi, G. A. Keeler, Y. Yang, J. Reno, G. M. Peake, F. Setzpfandt, I. Staude, T. Pertsch, and I. Brener, Nano Lett. **16**, 5426 (2016).
13. R. Camacho-Morales, M. Rahmani, S. Kruk, L. Wang, L. Xu, D. A. Smirnova, A. S. Solntsev, A. Miroshnichenko, H. H. Tan, F. Karouta, S. Naureen, K. Vora, L. Carletti, C. De Angelis, C. Jagadish, Y. S. Kivshar, and D. N. Neshev, Nano Lett. (2016).
14. G. Grinblat, Y. Li, M. P. Nielsen, R. F. Oulton, and S. A. Maier, ACS Nano **11**, 953 (2017).
15. D. Rocco, V. Gili, L. Ghirardini, L. Carletti, I. Favero, A. Locatelli, G. Marino, D. Neshev, M. Celebrano, M. Finazzi, G. Leo, and C. De Angelis, Photonics Res. **6**, B6 (2018).
16. L. Carletti, K. Koshelev, C. De Angelis, and Y. Kivshar, Phys. Rev. Lett. **121**, 033903 (2018).
17. L. Carletti, A. Locatelli, D. Neshev, and C. De Angelis, ACS Photonics **3**, 1500 (2016).
18. J. D. Sautter, L. Xu, A. E. Miroshnichenko, M. Lysevych, I. Volkovskaya, D. A. Smirnova, R. Camacho-Morales, K. Zangeneh Kamali, F. Karouta, K. Vora, H. H. Tan, M. Kauranen, I. Staude, C. Jagadish, D. N. Neshev, and M. Rahmani, Nano Lett. **19**, 3905 (2019).
19. D. Rocco, C. Gigli, L. Carletti, G. Marino, M. A. Vincenti, G. Leo, and C. De Angelis, IEEE Photonics J. **12**, 1 (2020).
20. A. Forouzmand, M. M. Salary, G. Kafaie Shirmanesh, R. Sokhoyan, H. A. Atwater, and H. Mosallaei, Nanophotonics **8**, 415 (2019).
21. D. Rocco, L. Carletti, R. Caputo, M. Finazzi, M. Celebrano, and C. De Angelis, Opt. Express **28**, 12037 (2020).
22. A. E. Minovich, A. E. Miroshnichenko, A. Y. Bykov, T. V. Murzina, D. N. Neshev, and Y. S. Kivshar, Laser & Photonics Rev. **9**, 195 (2015).
23. D. G. Baranov, S. V. Makarov, A. E. Krasnok, P. A. Belov, and A. Alù, Laser & Photonics Rev. **10**, 1009 (2016).
24. E. Klopfer, M. Lawrence, D. R. Barton, J. Dixon, and J. A. Dionne, Nano Lett. **20**, 5127 (2020).
25. M. R. Shcherbakov, P. P. Vabishchevich, A. S. Shorokhov, K. E. Chong, D.-Y. Choi, I. Staude, A. E. Miroshnichenko, D. N. Neshev, A. A. Fedyanin, and Y. S. Kivshar, Nano Lett. **15**, 6985 (2015).
26. G. Grinblat, H. Zhang, M. P. Nielsen, L. Krivitsky, R. Berté, Y. Li, B. Tilmann, E. Cortés, R. F. Oulton, A. I. Kuznetsov, and S. A. Maier, Sci. Adv. **6**, eabb3123 (2020).
27. D. Werdehausen, X. G. Santiago, S. Burger, I. Staude, T. Pertsch, C. Rockstuhl, and M. Decker, Adv. Theory Simulations **3**, 2000192 (2020).
28. L. Ghirardini, L. Carletti, V. Gili, G. Pellegrini, L. Duò, M. Finazzi, D. Rocco, A. Locatelli, C. De Angelis, I. Favero, M. Ravaro, G. Leo, A. Lemaître, and M. Celebrano, Opt. Lett. **42**, 559 (2017).
29. S. S. Kruk, R. Camacho-Morales, L. Xu, M. Rahmani, D. A. Smirnova, L. Wang, H. H. Tan, C. Jagadish, D. N. Neshev, and Y. S. Kivshar, Nano Lett. **17**, 3914 (2017).
30. M. Guasoni, L. Carletti, D. Neshev, and C. De Angelis, IEEE J. Quantum Electron. **53**, 1 (2017).
31. S. Danesi, M. Gandolfi, L. Carletti, N. Bontempi, C. De Angelis, F. Banfi, and I. Alessandri, Phys. Chem. Chem. Phys. **20**, 15307 (2018).
32. T. Skauli, P. Kuo, K. Vodopyanov, T. Pinguet, O. Levi, L. Eyres, J. Harris, M. Fejer, B. Gerard, L. Becouarn *et al.*, J. Appl. Phys. **94**, 6447 (2003).

FULL REFERENCES

1. N. I. Zheludev and Y. S. Kivshar, "From metamaterials to metadevices," Nat. Mater. **11**, 917–924 (2012).
2. M. Kadic, G. W. Milton, M. van Hecke, and M. Wegener, "3D metamaterials," Nat. Rev. Phys. **1**, 198–210 (2019).
3. N. Yu and F. Capasso, "Flat optics with designer metasurfaces," Nat. Mater. **13**, 139–150 (2014).
4. A. I. Kuznetsov, A. E. Miroshnichenko, M. L. Brongersma, Y. S. Kivshar, and B. Lukyanchuk, "Optically resonant dielectric nanostructures," Science **354**, aag2472 (2016).
5. Z. Zhou, J. Li, R. Su, B. Yao, H. Fang, K. Li, L. Zhou, J. Liu, D. Stellinga, C. P. Reardon, T. F. Krauss, and X. Wang, "Efficient silicon metasurfaces for visible light," ACS Photonics **4**, 544–551 (2017).
6. I. Brener, S. Liu, I. Staude, J. Valentine, and C. L. Holloway, *Dielectric metamaterials: fundamentals, designs and applications* (1st ed. Woodhead Publishing, 2019).
7. A. Krasnok, M. Tymchenko, and A. Alù, "Nonlinear metasurfaces: a paradigm shift in nonlinear optics," Mater. Today **21**, 8 – 21 (2018).
8. K. Koshelev, S. Kruk, E. Melik-Gaykazyan, J.-H. Choi, A. Bogdanov, H.-G. Park, and Y. Kivshar, "Subwavelength dielectric resonators for nonlinear nanophotonics," Science **367**, 288–292 (2020).
9. M. R. Shcherbakov, D. N. Neshev, B. Hopkins, A. S. Shorokhov, I. Staude, E. V. Melik-Gaykazyan, M. Decker, A. A. Ezhov, A. E. Miroshnichenko, I. Brener, A. A. Fedyanin, and Y. S. Kivshar, "Enhanced Third-Harmonic Generation in Silicon Nanoparticles Driven by Magnetic Response," Nano Lett. **14**, 6488–6492 (2014).
10. L. Carletti, A. Locatelli, O. Stepanenko, G. Leo, and C. De Angelis, "Enhanced second-harmonic generation from magnetic resonance in AlGaAs nanoantennas," Opt. Express **23**, 26544–26550 (2015).
11. V. Gili, L. Carletti, A. Locatelli, D. Rocco, M. Finazzi, L. Ghirardini, I. Favero, C. Gomez, A. Lemaître, M. Celebrano, C. De Angelis, and G. Leo, "Monolithic AlGaAs second-harmonic nanoantennas," Opt. Express **24**, 15965–15971 (2016).
12. S. Liu, M. B. Sinclair, S. Saravi, G. A. Keeler, Y. Yang, J. Reno, G. M. Peake, F. Setzpfandt, I. Staude, T. Pertsch, and I. Brener, "Resonantly Enhanced Second-Harmonic Generation Using III–V Semiconductor All-Dielectric Metasurfaces," Nano Lett. **16**, 5426–5432 (2016).
13. R. Camacho-Morales, M. Rahmani, S. Kruk, L. Wang, L. Xu, D. A. Smirnova, A. S. Solntsev, A. Miroshnichenko, H. H. Tan, F. Karouta, S. Naureen, K. Vora, L. Carletti, C. De Angelis, C. Jagadish, Y. S. Kivshar, and D. N. Neshev, "Nonlinear Generation of Vector Beams From AlGaAs Nanoantennas," Nano Lett. (2016).
14. G. Grinblat, Y. Li, M. P. Nielsen, R. F. Oulton, and S. A. Maier, "Efficient Third Harmonic Generation and Nonlinear Subwavelength Imaging at a Higher-Order Anapole Mode in a Single Germanium Nanodisk," ACS Nano **11**, 953–960 (2017).
15. D. Rocco, V. Gili, L. Ghirardini, L. Carletti, I. Favero, A. Locatelli, G. Marino, D. Neshev, M. Celebrano, M. Finazzi, G. Leo, and C. De Angelis, "Tuning the second-harmonic generation in algaas nanodimers via non-radiative state optimization [invited]," Photonics Res. **6**, B6–B12 (2018).
16. L. Carletti, K. Koshelev, C. De Angelis, and Y. Kivshar, "Giant Nonlinear Response at the Nanoscale Driven by Bound States in the Continuum," Phys. Rev. Lett. **121**, 033903 (2018).
17. L. Carletti, A. Locatelli, D. Neshev, and C. De Angelis, "Shaping the Radiation Pattern of Second-Harmonic Generation from AlGaAs Dielectric Nanoantennas," ACS Photonics **3**, 1500–1507 (2016).
18. J. D. Sautter, L. Xu, A. E. Miroshnichenko, M. Lysevych, I. Volkovskaya, D. A. Smirnova, R. Camacho-Morales, K. Zangeneh Kamali, F. Karouta, K. Vora, H. H. Tan, M. Kauranen, I. Staude, C. Jagadish, D. N. Neshev, and M. Rahmani, "Tailoring Second-Harmonic Emission from (111)-GaAs Nanoantennas," Nano Lett. **19**, 3905–3911 (2019).
19. D. Rocco, C. Gigli, L. Carletti, G. Marino, M. A. Vincenti, G. Leo, and C. De Angelis, "Vertical Second Harmonic Generation in Asymmetric Dielectric Nanoantennas," IEEE Photonics J. **12**, 1–7 (2020).
20. A. Forouzmand, M. M. Salary, G. Kafaie Shirmanesh, R. Sokhoyan, H. A. Atwater, and H. Mosallaei, "Tunable all-dielectric metasurface for phase modulation of the reflected and transmitted light via permittivity tuning of indium tin oxide," Nanophotonics **8**, 415–427 (2019).
21. D. Rocco, L. Carletti, R. Caputo, M. Finazzi, M. Celebrano, and C. De Angelis, "Switching the second harmonic generation by a dielectric metasurface via tunable liquid crystal," Opt. Express **28**, 12037–12046 (2020).
22. A. E. Minovich, A. E. Miroshnichenko, A. Y. Bykov, T. V. Murzina, D. N. Neshev, and Y. S. Kivshar, "Functional and nonlinear optical metasurfaces: Optical metasurfaces," Laser & Photonics Rev. **9**, 195–213 (2015).
23. D. G. Baranov, S. V. Makarov, A. E. Krasnok, P. A. Belov, and A. Alù, "Tuning of near- and far-field properties of all-dielectric dimer nanoantennas via ultrafast electron-hole plasma photoexcitation," Laser & Photonics Rev. **10**, 1009–1015 (2016).
24. E. Klopfer, M. Lawrence, D. R. Barton, J. Dixon, and J. A. Dionne, "Dynamic Focusing with High-Quality-Factor Metalenses," Nano Lett. **20**, 5127–5132 (2020).
25. M. R. Shcherbakov, P. P. Vabishchevich, A. S. Shorokhov, K. E. Chong, D.-Y. Choi, I. Staude, A. E. Miroshnichenko, D. N. Neshev, A. A. Fedyanin, and Y. S. Kivshar, "Ultrafast All-Optical Switching with Magnetic Resonances in Nonlinear Dielectric Nanostructures," Nano Lett. **15**, 6985–6990 (2015).
26. G. Grinblat, H. Zhang, M. P. Nielsen, L. Krivitsky, R. Berté, Y. Li, B. Tilmann, E. Cortés, R. F. Oulton, A. I. Kuznetsov, and S. A. Maier, "Efficient ultrafast all-optical modulation in a nonlinear crystalline gallium phosphide nanodisk at the anapole excitation," Sci. Adv. **6**, eabb3123 (2020).
27. D. Werdehausen, X. G. Santiago, S. Burger, I. Staude, T. Pertsch, C. Rockstuhl, and M. Decker, "Modeling optical materials at the single scatterer level: The transition from homogeneous to heterogeneous materials," Adv. Theory Simulations **3**, 2000192 (2020).
28. L. Ghirardini, L. Carletti, V. Gili, G. Pellegrini, L. Duò, M. Finazzi, D. Rocco, A. Locatelli, C. De Angelis, I. Favero, M. Ravaro, G. Leo, A. Lemaître, and M. Celebrano, "Polarization properties of second-harmonic generation in AlGaAs optical nanoantennas," Opt. Lett. **42**, 559–562 (2017).
29. S. S. Kruk, R. Camacho-Morales, L. Xu, M. Rahmani, D. A. Smirnova, L. Wang, H. H. Tan, C. Jagadish, D. N. Neshev, and Y. S. Kivshar, "Nonlinear Optical Magnetism Revealed by Second-Harmonic Generation in Nanoantennas," Nano Lett. **17**, 3914–3918 (2017).
30. M. Guasoni, L. Carletti, D. Neshev, and C. De Angelis, "Theoretical Model for Pattern Engineering of Harmonic Generation in All-Dielectric Nanoantennas," IEEE J. Quantum Electron. **53**, 1–5 (2017).
31. S. Danesi, M. Gandolfi, L. Carletti, N. Bontempi, C. De Angelis, F. Banfi, and I. Alessandri, "Photo-induced heat generation in non-plasmonic nanoantennas," Phys. Chem. Chem. Phys. **20**, 15307–15315 (2018).
32. T. Skauli, P. Kuo, K. Vodopyanov, T. Pinguet, O. Levi, L. Eyres, J. Harris, M. Fejer, B. Gerard, L. Becouarn *et al.*, "Improved dispersion relations for GaAs and applications to nonlinear optics," J. Appl. Phys. **94**, 6447–6455 (2003).